AUTOMATIC CORN PLANT POPULATION MEASUREMENT USING MACHINE VISION

D. S. Shrestha, B. L. Steward

ABSTRACT. *A machine vision–based corn plant population sensing system was developed to measure early growth stage corn population. Video was acquired from a vehicle–mounted digital video camera at V3 to V4 stages under different daylight conditions. Algorithms were developed to sequence video frames and to segment, singulate, and count corn plants. Vegetation segmentation was accomplished using a truncated ellipsoidal decision surface. Two features were extracted from each pixel row of the segmented images: total number of plant pixels, and their median position. Adjacent rows of the same class were grouped together and iteratively refined for final plant counting. Performance of this system was evaluated by comparing its estimation of plant counts with manual stand counts in 60 experimental units of 6.1 m sections of corn rows. The number of corn plants in these experimental units ranged from 14 to 48, corresponding to a population of 30,000 to 103,000 plants /ha. In low–weed field conditions, the system plant count was well correlated to manual stand count (R^2 = 0.90). Standard error of population estimate was 1.8 plants over 33.2 mean manual plant count, or 5.4% coefficient of variation.*

Keywords. *Corn, Image processing, Machine vision, Plant population, Precision agriculture, Video camera.*

Corn plant populations that are higher or lower than optimal can reduce crop yield. Duncan (1958) found that corn yield was maximized at particular plant populations depending on nutrient availability. Wiley and Heath (1969) investigated the relationships established by different researchers between corn population density and yield and found that the predictions had similar trends of yield maximization at particular plant population densities. Duncan (1984) pre–sented the theory of crowding as a reason for yield reduction. However, optimum plant densities have not been constant over time but have increased substantially over the last several decades (Troyer and Rosenbrook, 1983; Nafziger, 1994).

Even if a corn variety is planted at its optimal population, row spacing and interplant distance within a row can also affect the final yield. Plant population density, as well as interplant distribution, is important in effective utilization of available resources like nutrients and sunlight. Barbieri et al. (2000) studied the row spacing effect at different levels of nitrogen availability in corn. They found that the corn yield was higher when the row spacing was decreased for the same population density. The relative yield increase was higher for nitrogen–deficient fields. Doerge et al. (2002) measured spacing of 6,000 plants in research conducted in Missouri, Iowa, and Minnesota. The whole–field plant spacing standard deviation ranged from 3.2 to 6.9 inches. They estimated that every inch reduction in plant spacing standard deviation in a commercial field would increase the yield by about 3.4 bu/acre. Nafziger (1996) found that when there is a missing plant, the plants on either side compensated for only 47% of the reduced yield in lower population density fields (18,000 plants /acre) and 19% in higher plant density (30,000 plants/acre) fields, hence decreasing the final yield.

There are three main causes of variability in plant spacing: seed germination, planter seed placement, and plant death. Seed germination rates typically range from 90% to 95% (Nielsen, 2001). Planter performance depends both on planter maintenance and speed. Nielsen (1995) reported that when the planter speed varied from 6.4 to 11.2 km/h (4 to 7 mph), the planted seed rate at higher speeds was significantly different than the planted seed rate at lower speeds. He concluded that a yield loss of at least 1.9 bu/acre occurs at every 1 mph speed increase in the range of 4 to 7 mph. Weather– and pest–related damage may result in unevenly spaced plant survivors within a row (Nielsen, 2001). Because of these factors, established plant population and spacing may be different than target plant population.

Bullock et al. (1998) found that for variable–rate seeding to be profitable, a farmer needs extensive knowledge of site–specific plant population versus yield data from many years. Manual stand counts would not be feasible for a large field and are also susceptible to human error. An automated plant counting system provides a method for counting plants quickly and objectively. In addition, comparison of early stage plant population measurements with populations at harvest can be used to measure the plant survival rate throughout the growing period. Plant survival rates could be used to estimate the population density required at planting

Article was submitted for review in January 2002; approved for publication by the Information & Electrical Technologies Division of ASAE in December 2002.

Journal paper of the Iowa Agriculture and Home Economics Experiment Station, Ames, Iowa, Project No. 6, supported by Hatch Act and State of Iowa funds. The use of trade names is only meant to provide specific information to the reader and does not constitute endorsement by Iowa State University.

The authors are **Dev Sagar Shrestha,** Graduate Research Assistant, and **Brian L. Steward,** Assistant Professor, Department of Agricultural and Biosystems Engineering, Iowa State University, Ames, Iowa. **Corresponding author:** Brian L. Steward, Iowa State University, 206 Davidson, Ames, IA 50011; phone: 515–294–1452; fax: 515–294–2255; e–mail: bsteward@iastate.edu.

  ISSN 0001–2351

time to achieve the desired population density at harvesting time.

Because of the importance of plant population density and spacing distribution to produce the optimum yield, several researchers have investigated population measurement systems. Most population sensing technologies have been developed for application at harvest. Birrell and Sudduth (1995) and Sudduth et al. (2000) developed a combine–mounted mechanical sensor to map corn population at harvest. Plattner and Hummel (1996) developed another corn population sensor using non–contact optical sensors at harvest. Nichols (2000) also developed a corn population sensor using a moisture sensor to count corn stalks as they are pulled into the combine head. Easton and Easton (1996) developed a mechanical sensing system for counting young corn plants, which was mounted on a one–wheeled, human–powered cart.

With current advances in digital video technology, machine vision has potential as a sensing technology for corn plant population measurements. In addition, a machine vision system could be extended to measure other field variables like plant color, soil color, plant height, and other crop characteristics. Therefore, machine vision was investigated as a means to sense corn plant population.

Automated plant counting using machine vision involves three major steps. First, the individual video frames must be separated and the amount of overlap of the scene in two subsequent frames must be determined in order to avoid multiple counting of plants that occur in two frames. Second, the plants must be segmented from the scene background. Third, plants must be singulated and counted.

The objective of this research was to develop a machine vision sensing system for counting corn population at an early growth stage ranging from V3 to V4. Specific research objectives were to:

- Develop an image correspondence methodology for video frame sequencing that could reliably find the amount of shift from one frame image to the next in a video of field scenes.
- Develop a corn plant segmentation and singulation algorithm that would accurately estimate corn plant population over row lengths.

METHODOLOGY

EXPERIMENTAL SETTING

Two weeks after plant emergence, video sequences were collected in corn plots planted on 26 April 2001 (Asgrow RX686RR) at the Iowa State University Agronomy and Agricultural Engineering Research Center in Boone, Iowa. A Sony DCR–TRV900 digital camcorder was mounted on a John Deere Gator utility vehicle at 0.60 m above the ground with a 0.30 × 0.40 m field of view. Each captured image size was 480 × 720 pixels with 24–bit color resolution. The vehicle was driven over a corn row in a straight line with the camera directly over the plants at a speed of about 1 m/s. The shutter speed was adjusted to 1/1000 second, frames were captured in progressive scan mode, and other camera settings were set to auto. In the field, the video stream was recorded on a miniDV tape.

The corn plants were at V3 to V4 growth stages, which are the vegetative growth stages of corn when the third or fourth leaf collar is visible. The corn row spacing was 0.76 m (30 in.), and the target population was 74,000 plants/ha (30,000 plants per acre). Corn rows were divided into 6.1 m (20 ft) long sections by staking yellow construction tape perpendicular to the row direction. Each 6.1 m long corn row section was considered to be an experimental unit, and a total of 60 experimental units were used in the study. This length represented a trade–off between population measurement resolution and spatial sampling resolution. In addition, 6.1 m row sections are slightly longer than the row length recommended to achieve the recommended 1/1000–acre stand counts for 0.76 m (30 in.) rows (Benson, 1990). The number of plants within each experimental unit was determined through manual stand counts.

In the laboratory, video streams were transmitted from the camera to a personal computer using an IEEE 1394 serial interface. Adobe Premiere 6 (San Jose, Cal.) was used to capture the video stream as AVI files and then to decompress and store individual frames as color tagged image file format (TIFF) files. Matlab Ver. 6 (The Mathworks, Inc., Natick, Mass.) was used for development of image processing algorithms and subsequent image processing.

IMAGE SEQUENCING

Image sequencing is the process of determining the amount of overlap in succeeding video frames. This is essentially an image correspondence problem in which common scene points in two images are identified and matched. There are many methods available in the literature for image correspondence. One technique is to match a pattern and a searched image through the use of a matching criterion that serves as a measure of correlation (Sonka et al., 1998). Feature–based image correspondence, such as the method developed by Dai and Khorram (1999), is another possible approach for matching remotely sensed image pairs. Their algorithm included image segmentation, control–point selection and correspondence, and transformation parameter estimation. In general, for the feature–based algorithms to be effective, images should contain objects with well–defined shapes and edges, like a river or road, as are usually encountered in remote sensing. Feature–based algorithms also tend to be computationally expensive. For cornfield scenes, the objects are not well defined. In addition, the computation time must be constrained due to the large number of frames to be sequenced. Sanchiz et al. (1995) developed a feature–based system to sequence the video frames in fields containing small cabbage plants with the assumption that there is no movement in the scene itself. In our case, however, the corn plant leaves were moving in the wind, and inclusion of plant regions in the correspondence algorithm produced erroneous results.

Image correspondence can be done both in spatial and frequency domains. In the frequency domain, image correspondence can be obtained to sub–pixel accuracy, but the computational cost is higher than spatial correlation–based image matching (Averbuch and Keller, 2002). Correspondence is a key problem in machine vision applications and no general reliable solution exists (Maciel and Costeira, 2002).

In this research, to accomplish image sequencing, intensity images were derived from color images, and the amount of shift between sequential frames was estimated. Assuming that camera rotation was negligible from frame to frame, the image sequencing problem consisted of finding the shift in the next frame relative to the current frame being processed. A patch was selected randomly in the current frame with the constraint that its expected corresponding matching location (search region) was within the boundary of the next frame. A 30 × 30 pixel patch was selected as a balance between two competing criteria: to minimize computation time and to maximize textural content, which both increase with patch size. This patch size corresponded to 1.88 cm in the direction of travel and 1.67 cm perpendicular to the direction of travel.

When selecting a patch in the current frame for matching with the next frame, the anticipated shift was taken into account so that the search region in the next frame completely lay within the next frame boundary (fig. 1). The search region was set such that the patch could be moved by 30 pixels in any direction from the anticipated amount of shift. The average shift of two previous images was used to determine the anticipated shift amount. Once a patch in the current frame and the corresponding search region were selected, both patch and search region were searched for vegetation by segmenting plants using the truncated ellipsoid method, described in the next section. If more than 5% of the pixels in either the patch or the search region were classified as vegetation, then that patch selection was disqualified from further processing. In addition, if the patch was very dark (average intensity < 0.2) or very bright (average intensity > 0.8), then the patch was disqualified and another patch was reselected randomly. Plant regions were excluded because the position of a plant may change from frame to frame due to wind moving the leaves, leading to a false match. If the intensity of a patch was too high, generally it was too saturated to contain texture information. Similarly, dark patches usually had a low level of information.

For the first two images in a sequence, there was no information available for the anticipated shift. Therefore, to determine the amount of shift between the first and the second frame in the sequence, it was assumed that the vehicle always traveled forward, and the patch was selected within the lower 100 rows of the first frame within a 50–column margin from both right and left sides. The entire second frame was then searched for the match location of that patch.

If the patch was $m \times n$ pixels and the search region was M × N pixels, the matching error for each position was determined by:

$$\mathrm{Err}_{p,q} = \sum_{i=1}^{n}\sum_{j=1}^{m}\left|\mathrm{P}_{i,j} - \mathrm{S}_{i+p-1,\,j+q-1}\right| \tag{1}$$

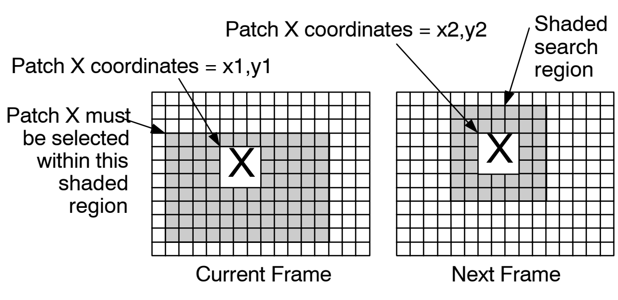

Figure 1. For image sequencing, an image patch (X) in the current frame was shifted in a search region in the next frame to find the best match. The difference in coordinates of the patch matched to the second frame gives the amount of shift from the current frame to the next frame.

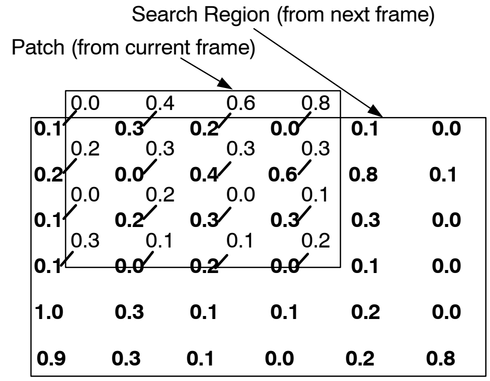

Figure 2. Process of calculating an error matrix (Err). The patch was shift over the search region. For the position shown above $\mathrm{Err}_{1,1} = |(0.0 - 0.1)| + |(0.4 - 0.3)| + \ldots + |(0.2 - 0.0)| = 3.3$.

where Err is the $(\mathrm{M} - m) \times (\mathrm{N} - n)$ error matrix. The (p,q) term of Err corresponds to the sum of absolute errors when the patch was shifted by (p,q) pixels from the upper left corner of the search region. P is the intensity patch from the current frame, and S is the search region from the next frame (fig. 2).

A candidate match was found by finding the minimum valued element in Err. To determine the validity of a match, the minimum value of Err had to be significantly lower than other values (fig. 3). In order to test for a statistically significant minimum, the values in Err were sorted in ascending order, and the difference between successive values was calculated. For a valid match, the difference between the lowest error and the next to the lowest error value was required to be higher than five standard deviations (5σ) from the mean of the remaining error differences. For example, the error matrix for figure 2 was calculated as:

$$\mathrm{Err} = \begin{vmatrix} 3.3 & 4.3 & 4.3 \\ 2.8 & 0.0 & 3.0 \\ 4.1 & 2.6 & 3.8 \end{vmatrix} \tag{2}$$

The matrix Err was rearranged in a row of ascending values, and the difference ΔErr was calculated as:

$$\Delta\mathrm{Err} = [2.6 \quad 0.2 \quad 0.2 \quad 0.3 \quad 0.5 \quad 0.3 \quad 0.2 \quad 0.0] \tag{3}$$

Since the first value of ΔErr (i.e., 2.6) is more than five standard deviations from the mean of the rest of the differences, the minimum error (0.0) in the Err matrix was considered to be a true minimum, and the match was accepted. If a valid match, based on a 5σ criterion, could not be found in the specific region, then another random patch was chosen in the current frame and searching was repeated. This criterion was established from Chebyshev's theorem, which applies to any distribution (Walpole and Myers, 1978) and shows that the minimum probability of a correct match is given by:

$$\mathrm{P} \geq 1 - \frac{1}{5^2} = 0.96 \tag{4}$$

where P is the probability that the value of the random variable will be less than five standard deviations from the mean. Thus, for error differences that are more than five standard deviations from the mean, there is at most a 4% probability that the match was due to a random minimum in the error matrix.

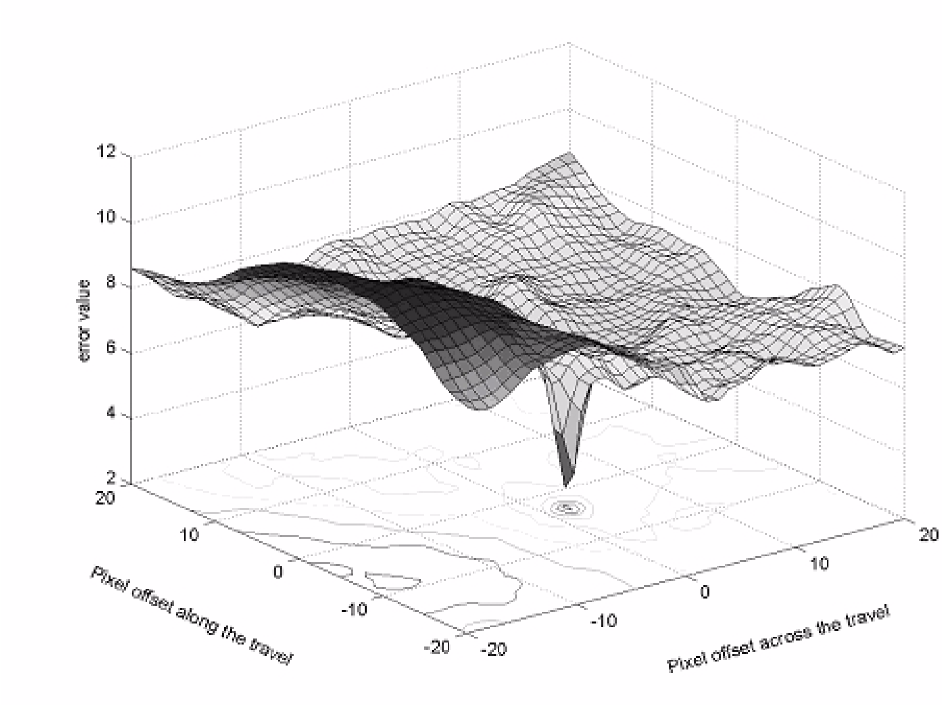

Figure 3. Example of an error surface and its contour for a typical patch matching. The minimum error value must be significantly different from the mean error to be accepted as a valid match.

Image Segmentation

The next step after image correspondence was segmentation of vegetation from background. Different methods are available for separating vegetation from non–vegetation regions. Meyer et al. (1998) segmented plant and background by thresholding the excess green color index. Andreasen et al. (1997) segmented images by thresholding the median filtered histogram of the green chromaticity coordinates. Pérez et al. (2000) used a normalized difference index (NDI) along with morphological operations for plant segmentation. The segmentation algorithm employed in this research should be able to segment the plant in changing lighting conditions that occur in the field due to clouds and the time of the day.

Tian and Slaughter (1998) developed an algorithm to achieve segmentation robustness in outdoor field images under varying lighting conditions. This algorithm was based on cluster analysis of pixels in color space for labeling pixels and Bayesian classification for the development of a decision surface in color space. The segmentation method used for this research employed a decision surface in color space that was defined by only three parameters (Shrestha et al., 2001). This surface was a truncated ellipsoidal surface given by:

$$\frac{R^2}{D^2}+\frac{(1-G)^2}{(E\times B+F)^2}=1 \tag{5}$$

where R, G, and B were the red, green, and blue intensities ranging from 0 to 1, and D, E, and F were the parameters describing the shape of the ellipsoid. Each of these parameters has a physical meaning based on the perceived green region in color space. D is the maximum red intensity still perceived green when B = 0 and G =1. E is the slope of the ellipsoid boundary in the green–blue plane. F is the distance from maximum to minimum green intensity that is perceived green when both blue and red channels are zero (fig. 4). Constant parameter values D = 0.9, E = –0.57, and F = 0.81 were used for image segmentation in this research. These parameter values were determined by Shrestha et al. (2001) to provide a general segmentation of plants across varying outdoor lighting conditions. For a given pixel color vector, the pixels were classified according to the decision rule:

$$\frac{R^2}{D^2}+\frac{(1-G)^2}{(E\times B+F)^2}\ \underset{\omega_2}{\overset{\omega_1}{\gtrless}}\ 1 \tag{6}$$

where ω_1 is the background class, and ω_2 is the vegetation class. Because the surface is only defined by three parameters, adjustments can easily be made as lighting conditions change. Adjustments of the surface parameters by a neural net have been investigated and are the topic of another article (Shrestha et al., 2001).

Plant Counting

After image sequencing and segmentation, images consisting of sequenced frames were analyzed to determine the number of plants and plant center locations. Jia and Krutz (1992) studied the feasibility of detecting main veins along leaves and found the intersecting point to estimate the corn plant center. At early growth stages, however, there were no consistent distinct veins observed in corn plant leaves. Therefore, it was not possible to use main veins for plant center detection.

In order to determine the plant centers and to count the plants, two features were extracted from every row of the binary segmented images: the total number of plant pixels in each image row, and the median position of the plant pixels along each row. Once all the image rows were scanned and

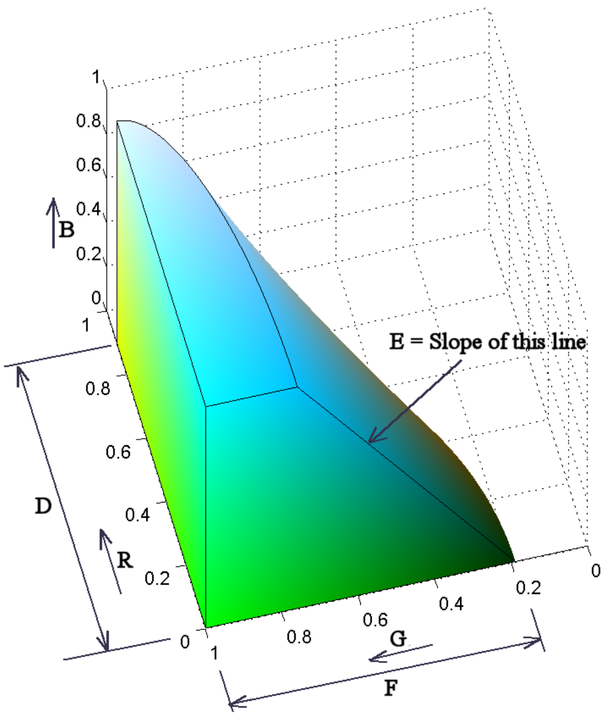

Figure 4. The truncated ellipsoidal decision surface in RGB color space used to segment vegetation from background. A pixel with RGB intensities inside the ellipsoid is considered a plant pixel. Parameter values used to segment plant from background were: D = 0.9, E = –0.57, and F = 0.81.

extracted features were recorded, a row was either classified as a plant row or a background row. An image row was classified as a plant row if:

1. The variation in median position of that row to the previous was less than the total number of plant pixels in that row, and:
2. The plant pixel count of that row was greater than the mean value of total plant pixels in each row across the entire experimental unit.

Once a frame sequence from an experimental unit had been initially classified, adjacent plant rows and background rows were grouped into plant or background regions, and the average length of plant and background regions were calculated. Plant center row locations were estimated to be the middle row of each plant region. The plant center column was the mean of the median positions for that region. This classification resulted in an initial estimate of the number of plants and plant center locations. Next, the plant and background regions were further refined using the following rule base:

- Plant regions that were less than 20% of the mean plant region length were considered to be false plant regions and were reclassified as background.
- Background regions that were less than 20% of the mean background region length were considered to be false background regions and were reclassified as plant.
- Any plant center found outside a 5σ interval from the mean plant center position across the sequence was considered to be a weed, and thus the region is reclassified as background.

After this refinement, the plants were counted again. If the plant count varied by more than 5% of the original count, the plant and background statistics were updated, and the regions were refined again through the rule base. When the plant count varied by less than 5%, the algorithm stopped.

Finally, plant regions that were more than twice the length of an average plant region were counted as doubles, and those more than three times the length were counted as triples. The plant center row locations were assumed to be at the middle of the plant region. In cases of multiple plants, the center was assumed to be at the middle of each of the adjacent plant regions.

Experimental Design

Image Sequencing Performance

To evaluate the performance of the image sequencing algorithm, a video sequence of 50 images was processed with the algorithm. Processing was repeated 30 times. For each image pair, the number of failed patch and search region selection attempts, the number of attempts to achieve a significant match, and shifts along and across the direction of travel between subsequent frames were all recorded. The SAS (SAS Institute, Cary, N.C.) General Linear Model procedure (GLM) was used to test for significance differences in shifts statistics across replication of the algorithm and image pairs.

Plant Counting Performance

The plant count estimated by the sensing system was compared with that measured manually in 60 experimental units. Linear regression analysis was used to analyze the relationship between the two measurements. To determine the false plant and background region thresholds used in the algorithm, they were varied from 5% to 25% at 5% intervals. For each threshold combination, the plant counting algorithm was used to estimate the number of plants in 13 randomly chosen sequences. The estimated plant count was compared to the manual count, and a sum square of error statistic was calculated. The combination that minimized the error statistic was found and was used in the analysis of overall counting performance. The sensitivity of the algorithm's accuracy to the false plant and background thresholds as well as to the algorithm stopping criteria and distance from the crop row threshold were analyzed using all 60 experimental units. The plant count in each of 60 experimental units estimated by the sensing system was compared with that measured manually. Linear regression analysis was used to analyze the relationship between the two measurements.

Results and Discussion

Image Sequencing Performance

From the analysis of variance of the 50–frame sequence, the mean shift between two images along the direction of travel was 71.58 pixels, which, based on the camera field of view, would be a shift of 0.045 m of the field surface between two images. From this shift distance, the vehicle speed was estimated to be 1.34 m/s. At this speed, 85% of each frame is overlapped with the previous frame. There were significant differences in the mean pair–to–pair shifts in the travel direction ($P < 0.0001$). These differences were expected and are due primarily to variations in vehicle speed. After accounting for the pair–to–pair variation, the standard deviation in the shift estimation process was 2.3 pixels. This corresponded to 0.0014 m of the field surface or 3.2% of the mean shift. The modified Levene test (Conover et al., 1981) revealed significant differences in shift variance across image pairs ($P < 0.0001$). This finding indicated that the image correspondence algorithm was finding larger differences across replications of the algorithm in particular image pairs than in other image pairs. Since the location of the patches is random, correspondence of frame pairs may vary depending on the location of the patch. This variation is due partly to uneven depth to objects in the image scene and vehicle yaw across the pair, resulting in a rotation from one image to the next. The algorithm operated under the assumption of negligible frame–to–frame camera rotation, and based on these results, any error introduced because of this assumption was small.

The mean lateral shift between two images was 0.58 pixels, revealing that either the vehicle was turning or that the camera was slightly rotated relative to the centerline of the vehicle. After accounting for the pair–to–pair shift with the ANOVA model, the standard deviation of the shift estimation algorithm was 1.7 pixels. Once again, there were significant differences ($P < 0.0001$) in the shift variance across image pairs.

The number of attempts required to achieve a significant match ranged from 1 to 5 across the entire experiment. The mean was 1.21 attempts, and the standard deviation was 0.49 attempts. There were significant differences in the number of attempts ($P < 0.0001$), indicating that some image pairs tended to require more attempts than others. Upon further examination of these pairs, often one of the frame images was blurred, leading to difficulty in establishing a significant match. Nevertheless, even though on the average more matching attempts were required for blurred images than for a sharply focused image, significant matches were found for each of the pairs in the sequence. In addition, only 1.9% of the initial patch selections were rejected. A maximum number of two rejections before final patch selection occurred in 0.20% of the cases. Even when a randomly selected patch was valid, the initial search region selection was rejected 5% of the time, hence forcing the algorithm to reselect for a new patch. The search region area was nine times larger, so an increased likelihood of finding a plant region in a search region was expected.

Plant Counting Performance

Manual plant counts over the 60 corn row sections varied over a range of 14 to 48 plants with a mean value of 33.2 plants. Linear regression analysis resulted in a R^2 value of 0.90 (fig. 5). The slope and intercept of the regression line were 0.93 and 1.98, respectively, and were not significantly different from 1 and 0, respectively. The RMS error of plant counts estimated by the system was 1.8 plants over the 6.1 m length of a corn row. This error was 5.4% of the mean. Based on the manual counts, the local population in the corn row sections varied from 30,100 to 103,000 plants/ha (12,200 to 41,800 plants/acre). Measuring over a 6.1 m corn row with 0.71 m spacing resulted in a measurement resolution of ±2150 plants/ha, which was 3% of the target population.

From the analysis of the set of 13 sequences, the combination of a false plant region threshold of 20% of the mean plant region length and a false background region threshold of 20% of the mean background region length gave the least squared error. This combination was thus selected and used to count plants in all 60 experimental units in the analysis of overall system performance. System accuracy was sensitive to the false plant and background thresholds. However, an R^2 greater than 0.8 was found when the false plant threshold was within the range of 10% to 20% and that for false background was between 15% and 25% (fig. 6). A maximum R^2 of 0.9 occurred with the 20% to 20% threshold combination.

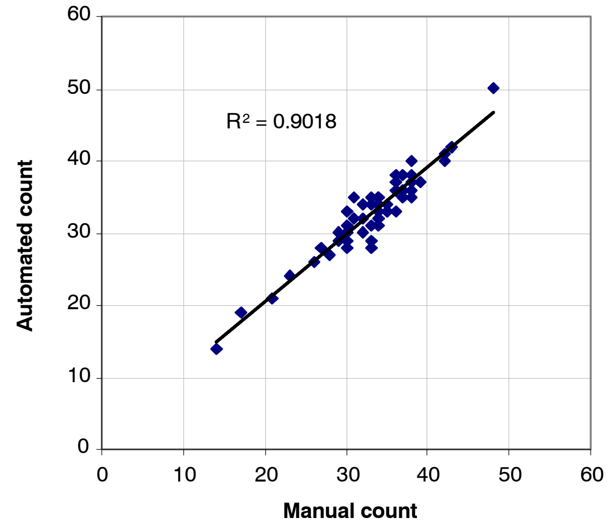

Figure 5. Regression of system–estimated counts onto manual counts for 60 experimental units. The regression had an R^2 of 0.9018 and an RMSE of 1.8 plants.

Plant count accuracy was not sensitive to variations in the threshold for excluding plant pixels. When this threshold was varied from 3 to 5 standard deviations away from mean row position, R^2 varied by 0.902 to 0.896. The plant count algorithm–stopping criterion was also varied to investigate its effect on the number of refinement iterations and counting accuracy. When a change in plant counts less than 5% was required, it took an average of 3.0 iterations before the refinement algorithm stopped. When the stopping criterion was increased to 10%, the mean number of iterations decreased to 2.53, but R^2 also decreased to 0.84. When the

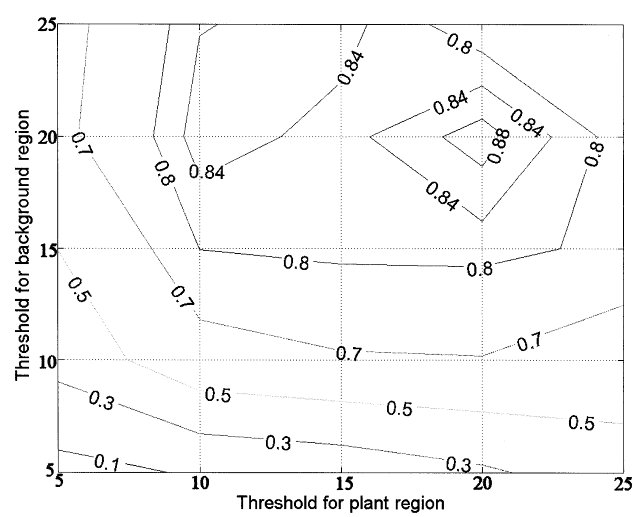

Figure 6. Contour plot of R^2 for different combinations of plant and background region thresholds. Thresholds between 10 and 20 for the plant region and thresholds between 15 and 25 for the background region produced $R^2 > 0.8$.

stopping criterion was changed to 1%, the mean number of iterations increased to 3.38 times before stopping, but R^2 only increased to 0.906. Therefore, the stopping criterion of 5% was found to be a suitable tradeoff between accuracy and time.

One of the main sources of error found was variability in plant size and leaf orientation within an experimental unit. This made the threshold used to refine the plant and background region sensitive to plant size distribution. More weed and noise pixels were counted as plants when the false plant region threshold was lowered below 20%, and small plants were considered to be weeds when the threshold was increased. However, under low–weed conditions and plant growth stages V3 to V4, the system was able to estimate the number of plants across in a 6.1 m row with an RMSE less than 3 plants over a range of parameters.

Conclusions

A patch–matching algorithm with criteria for region selection and match validity is a feasible method for sequencing the video frames of corn row scenes acquired by a commercial digital video camera on a vehicle moving at 1 to 2 m/s.

A plant–counting algorithm using two easily obtainable image features and a straightforward iterative rule base was able to achieve population measurement accuracies similar to the system measurement resolution.

References

Andreasen, C., M. Rudemo, and S. Sevestre. 1997. Assessment of weed density at an early stage by use of image processing. *Weed Research* 37: 5–18.

Averbuch, A., and Y. Keller. 2002. FFT–based image registration. In *International Conference on Acoustics, Speech, and Signal Processing* 4: 3608–3611. Piscataway, N.J.: IEEE.

Barbieri, P. A., H. R. Sainz Rozas, F. H. Andrade, and H. E. Echeverria. 2000. Row spacing effect at different levels of nitrogen availability in maize. *Agronomy J*. 92(2): 283–288.

Benson, G. O. 1990. Corn replant decisions: A review. *J. Production Agric*. 3(2): 180–184.

Birrell, S. J., and K. A. Sudduth. 1995. Corn population sensor for precision farming. ASAE Paper No. 951334. St. Joseph, Mich.: ASAE.

Bullock, D. G., D. S. Bullock, E. D. Nafziger, T. A. Doerge, S. R. Paszkiewicz, P. R. Carter, and T. A. Peterson. 1998. Does variable–rate seeding of corn pay? *Agronomy J*. 90(6): 830–836.

Conover, W. J., M. E. Johnson, and M. M. Johnson. 1981. A comparative study of tests for homogeneity of variances, with applications to the outer continental shelf bidding data. *Technometrics* 23(4): 351–361.

Dai, X., and S. Khorram. 1999. A feature–based image registration algorithm using improved chain–code representation combined with invariant moments. *IEEE Trans. Geoscience and Remote Sensing* 37(5): 2351–2362.

Doerge, T., T. Hall, and D. Gardner. 2002. New research confirms benefits of improved plant spacing in corn. *Crop Insights* 12(2): 1–5.

Duncan, W. G. 1958. The relationship between corn populations and yield. *Agronomy J*. 50: 82–84.

_____. 1984. A theory to explain the relationship between corn population and grain yield. *Crop Science* 24(6): 1141–1145.

Easton, D. T., and Easton, D. J. 1996. Device to measure and provide data for plant population and spacing variability. U.S. Patent No. 5,568,405.

Jia, J., and G. W. Krutz. 1992. Location of maize plant with machine vision. *J. Agric. Eng. Research* 52(3): 169–181.

Maciel, J., and J. Costeira. 2002. Robust point correspondence by concave minimization. *Image and Vision Computing* 20(9–10): 683–690.

Meyer, G. E., T. Mehta, M. F. Kocher, D. A. Mortensen, and A. Samal. 1998. Textural imaging and discriminant analysis for distinguishing weeds for spot spraying. *Trans. ASAE* 41(4): 1189–1197.

Nafziger, E. D. 1994. Corn planting date and plant population. *J. Production Agric*. 7(1): 59–62.

_____. 1996. Effects of missing and two–plant hills on corn grain yield. *J. Production Agric.* 9(2): 238–240.

Nichols, S. W. 2000. Method and apparatus for counting crops sensor. U.S. Patent No. 6,073,427.

Nielsen, R. L. 1995. Planting speed effects on stand establishment and grain yield of corn. *J. Production Agric.* 8(3): 391–393.

_____. 2001. Stand establishment variability in corn. AGRY–91–1 (Rev. Nov. 01). W. Lafayette, Ind.: Purdue University, Department of Agronomy.

Pérez, A. J., F. López, J. V. Benlloch, and S. Christensen. 2000. Colour and shape analysis techniques for weed detection in cereal fields. *Computers and Electronics in Agri*culture 25(3): 197–212.

Plattner, C. E., and J. W. Hummel. 1996. Corn plant population sensor for precision agriculture. In *Proc. 3rd International Conference on Precision Agriculture*, 785–794. P. C. Robert, R. H. Rust, and W. E. Larson, eds. Madison, Wisc.: ASA, CSSA, and SSSA.

Sanchiz, J. M., F. Pla, J. A. Marchant and R. S. Brivot. 1995. Structure from motion techniques applied to crop field mapping. *Image and Vision Computing* 14(5): 353–363.

Sonka, M., V. Hlavac, and R. Boyle. 1998. Segmentation. Chapter 5 in *Image Processing, Analysis and Machine Vision*, 190–193. Boston, Mass.: PWS Publishing.

Shrestha, D. S., B. Steward, and E. Bartlett. 2001. Segmentation of plant from background using neural network approach. In *Intelligent Engineering Systems through Artificial Neural Networks: Proc. Artificial Neural Networks in Engineering (ANNIE) International Conference*, 11: 903–908. New York, N.Y.: ASME Press.

Sudduth, K. A., S. J. Birrell, and M. J. Krumpelman. 2000. Field evaluation of a corn population. In *Proc. 5th International Conference on Precision Agriculture*, CD–ROM. T. C. Robert, R. H. Rust, and W. E. Larson, eds. Madison, Wisc.: ASA, CSSA, and SSSA.

Tian, L. F., and D. C. Slaughter. 1998. Environmentally adaptive segmentation algorithm for outdoor image segmentation. *Computers and Electronics in Agric*. 21(3): 153–168.

Troyer, A. F., and R. W. Rosenbrook. 1983. Utility of higher plant densities for corn performance testing. *Crop Science* 23(5): 863–867.

Walpole, R. E., and R. H. Myers. 1978. Random variables. Chapter 2 in *Probability and Statistics for Engineers and Scientists*, 72–75. 2nd ed. New York, N.Y.: Macmillan.

Wiley, R. W., and S. B. Heath. 1969. The quantitative relationship between plant population and crop yield. In *Advances in Agronomy* 21: 281–321. N. C. Brady, ed.